High precision determination of the Q^2 evolution of the Bjorken sum

A. Deur,[1] Y. Prok,[2,1] V. Burkert,[1] D. Crabb,[3] F.-X. Girod,[1] K. A. Griffioen,[4] N. Guler,[2,*]
S. E. Kuhn,[2] and N. Kvaltine[3]

[1]*Thomas Jefferson National Accelerator Facility, Newport News, Virginia 23606, USA*
[2]*Old Dominion University, Norfolk, Virginia 23529, USA*
[3]*University of Virginia, Charlottesville, Virginia 22904, USA*
[4]*College of William and Mary, Williamsburg, Virginia 23187, USA*
(Received 30 May 2014; published 18 July 2014)

We present a significantly improved determination of the Bjorken sum for $0.6 \leq Q^2 \leq 4.8$ GeV^2 using precise new g_1^p and g_1^d data taken with the CLAS detector at Jefferson Lab. A higher-twist analysis of the Q^2 dependence of the Bjorken sum yields the twist-4 coefficient $f_2^{p-n} = -0.064 \pm 0.009 \pm_{0.036}^{0.032}$. This leads to the color polarizabilities $\chi_E^{p-n} = -0.032 \pm 0.024$ and $\chi_B^{p-n} = 0.032 \pm 0.013$. The strong force coupling is determined to be $\alpha_s^{\overline{\rm MS}}(M_Z^2) = 0.1123 \pm 0.0061$, which has an uncertainty a factor of 1.5 smaller than earlier estimates using polarized deep inelastic scattering (DIS) data. This improvement makes the comparison between α_s extracted from polarized DIS and other techniques a valuable test of QCD.

I. INTRODUCTION

The Bjorken sum rule [1] is a cornerstone in the study of nucleon spin structure. It has been investigated via polarized deep inelastic scattering (DIS) at SLAC, CERN, DESY [2–8] and Jefferson Lab (JLab) [9–12]. In the limit of infinite squared four-momentum transfer Q^2 the sum rule is [1]

$$\Gamma_1^{p-n} \equiv \Gamma_1^p - \Gamma_1^n \equiv \int_0^1 dx(g_1^p(x) - g_1^n(x)) = \frac{g_A}{6}, \quad (1)$$

where g_1^p and g_1^n are the spin-dependent proton and neutron structure functions, respectively, g_A is the nucleon flavor-singlet axial charge, and x is the Bjorken scaling variable. At a finite Q^2 large enough so that partonic degrees of freedom are relevant, the Bjorken sum rule has been generalized to account for perturbative QCD (pQCD) radiative corrections (the leading-twist term) and non-perturbative power corrections (higher-twist terms). In the $\overline{\rm MS}$ scheme, the sum rule becomes [13]

$$\Gamma_1^{p-n} = \frac{g_A}{6}\left[1 - \frac{\alpha_s}{\pi} - 3.58\left(\frac{\alpha_s}{\pi}\right)^2 - 20.21\left(\frac{\alpha_s}{\pi}\right)^3 + \cdots\right] + \sum_{i=2,3\ldots}^{\infty} \frac{\mu_{2i}^{p-n}(Q^2)}{Q^{2i-2}}, \quad (2)$$

where the strong coupling α_s has itself the form of a perturbative series depending on Q^2, and the Q^2 dependence of the higher-twist coefficients $\mu_{2i}^{p-n}(Q^2)$ is calculable from pQCD. The logarithmic Q^2 dependence induced by

the pQCD radiative corrections that dominate for $\alpha_s \ll 1$ has allowed QCD to be established as the correct theory of the strong force. In turn, the higher-twist power corrections μ_{2i}/Q^{2i-2} characterize QCD in a stronger coupled regime with typically $\alpha_s > 0.3$. Here, at lower Q^2, partons start to interact strongly and react more and more coherently to the probing particles. Thus, the higher twists describe the transition between the partonic and hadronic degrees of freedom for the strong force.

The isovector nature of the Bjorken integral makes it a simpler quantity to understand theoretically than the integrals for the proton or neutron separately. This is particularly useful for nucleon structure calculations performed in different Q^2 ranges that reflect large or small α_s. These regimes, with their suitable calculation techniques, are summarized below.

   (i) For Q^2 above a few GeV^2, the partonic degrees of freedom are relevant. Here, pQCD can be tested through the leading-twist part of Eq. (2). The subtraction of Γ_1^n from Γ_1^p removes the nucleon matrix elements a_0 and a_8, and provides a rigorous QCD prediction. The subtraction also cancels the gluon and quark-singlet contributions to the Q^2 dependence of the sum rule.
   (ii) At intermediate Q^2 (from a few GeV^2 down to a few tenths of GeV^2), nonperturbative contributions affect the Q^2 dependence. Lattice QCD is the leading calculational technique in this regime. The isovector nature of Γ_1^{p-n} simplifies lattice calculations by removing all disconnected diagrams, which are CPU expensive to compute [14].
   (iii) At low Q^2 (below a few tenths of a GeV^2), chiral perturbation theory, which uses effective hadronic, rather than fundamental partonic, degrees of freedom, is applicable. The suppression of the Δ_{1232}

resonance contribution to Γ_1^{p-n} facilitates the chiral perturbation theory calculations, making these predictions more robust [15].

New data from the JLab CLAS EG1-DVCS experiment, taken on polarized proton and deuteron targets, have become available [16]. The kinematics of new data largely overlap the higher Q^2 coverage of earlier JLab data [9,11], but with smaller statistical errors. On the other hand, the previous JLab polarized data set covers lower Q^2 and higher x. Put together with these data, the EG1-DVCS data allow us to study the Bjorken sum at higher Q^2 and with improved statistical precision. Studies of the earlier data showed the necessity of precise measurements at moderately large Q^2, greater than $\simeq 2$ GeV^2, in order to extract higher twists, because of the small magnitude of their total contribution. As Eq. (2) suggests, it may seem to be beneficial to determine higher twists at lower Q^2 where the unmeasured low-x contribution to Γ_1^{p-n} is smaller, the data are more precise, and the higher twists are enhanced. However, in the standard perturbative approach, this may not be reliable due to the following effects:

(i) Higher-order twist effects at low Q^2 rise quickly and the short Q^2 range over which this rise occurs is too small to disentangle these higher twists.

(ii) There is an increasing uncertainty on the twist-2 part because the proximity of the Landau pole magnifies the uncertainty on α_s.

(iii) While higher-order leading-twist terms are necessary at low Q^2, the renormalon problem [17] jeopardizes the convergence of the series and increases the uncertainties due to truncations.

It is possible to avoid part of the difficulty by developing expressions for the Bjorken sum rule with better convergence properties, as explored in [18]. We will not pursue this

interesting path, and will instead remain consistent with the previous analyses [9,11,19], using the standard expansion, Eq. (2), since the higher Q^2 kinematics of EG1-DVCS are suited to this approach.

II. ANALYSIS

A. Bjorken sum

The extraction of g_1^p and g_1^d from the EG1-DVCS data is described in Ref. [16]. The Q^2 coverage and the integration limits are given in Table I. Since moments must be integrated over all x, a model must supplement the data at low x. We describe the model in the next section. The Q^2 values for Γ_1^p and Γ_1^d often differ slightly. When combining them into Γ_1^{p-n}, the Q^2 was chosen as the mean between the proton and deuteron Q^2 values, weighted by the statistical uncertainties on Γ_1^p and Γ_1^d. Both Γ_1^p and Γ_1^d were linearly interpolated to the common Q^2 before being combined into the Bjorken sum, $\Gamma_1^{p-n} = 2\Gamma_1^p - \Gamma_1^d/(1 - 1.5\omega_d)$, with $\omega_d = 0.05 \pm 0.01$ [20]. (Here, Γ^d is calculated as "per nucleus," not as "per nucleon.") The result for Γ_1^{p-n} is plotted in Fig. 1 together with data from the previous experiments conducted at SLAC [3,5], DESY [7], JLab [9–11], and CERN [8]. The elastic contribution ($x = 1$) is not included. Overall, the Q^2 behavior of Γ_1^{p-n} is smooth within systematic uncertainties. There is good agreement between the world data on Γ_1^{p-n} and EG1-DVCS, including cases where the neutron moment, Γ_1^n, is obtained from a ^{3}He target [4,7,9]. We also plot the leading-twist next-to-next leading order (NNLO) pQCD calculation based on Eq. (2) (gray band). The width of the band stems from the uncertainty in the strong coupling α_s.

TABLE I. Kinematic ranges and partial and full Bjorken sums. Columns 2 and 3 give the x ranges over which the proton and deuteron data are measured, respectively. Column 4 provides the partial sum $\Gamma_{1,\text{meas}}^{p-n}$ from EG1-DVCS. Column 5 gives the measured sum supplemented by a fit to earlier JLab data in the high-x domain, $\Gamma_{1,\text{meas+hi.}x}^{p-n}$. The experimental systematic uncertainty is denoted by $\sigma_{\text{meas}}^{\text{syst}}$. The high-$x$ interpolation is $\sigma_{\text{hi.}x}^{\text{syst}}$. Column 8 gives the total $\Gamma_{1,\text{tot}}^{p-n}$ sum, and σ^{syst} and σ^{stat} are the total (experimental, high-x and low-x) systematics and statistical uncertainties on $\Gamma_{1,\text{tot}}^{p-n}$, respectively. The ratio of the sum without the low-x estimate, $\Gamma_{1,\text{meas+hi.}x}^{p-n}$, over the total is given by $\Gamma_{1,\text{meas+hi.}x}^{p-n}/\Gamma_{1,\text{tot}}^{p-n}$.

| Q^2 (GeV^2)	x range (p)	x range (d)	$\Gamma_{1,\text{meas}}^{p-n}$	$\Gamma_{1,\text{meas+hi.}x}^{p-n}$	$\sigma_{\text{meas}}^{\text{syst}}$	$\sigma_{\text{hi.}x}^{\text{syst}}$	$\Gamma_{1,\text{tot}}^{p-n}$	σ^{syst}	σ^{stat}	$\Gamma_{1,\text{meas+hi.}x}^{p-n}/\Gamma_{1,\text{tot}}^{p-n}$
0.600	0.0695–0.072	0.070–0.074	−0.0001	0.0612	0.0001	0.0029	0.0940	0.0048	0.0005	0.651
0.698	0.0795–0.091	0.081–0.094	0.0031	0.0670	0.0002	0.0054	0.1056	0.0068	0.0005	0.634
0.840	0.0970–0.119	0.099–0.123	0.0079	0.0707	0.0004	0.0079	0.1164	0.0089	0.0006	0.607
0.972	0.110–0.155	0.113–0.168	0.0110	0.0674	0.0008	0.0088	0.1210	0.0099	0.0007	0.557
1.184	0.136–0.210	0.139–0.228	0.0169	0.0628	0.0016	0.0093	0.1257	0.0105	0.0007	0.500
1.361	0.151–0.304	0.168–0.322	0.0414	0.0606	0.0036	0.0082	0.1358	0.0103	0.0009	0.446
1.590	0.179–0.494	0.189–0.494	0.0580	0.0642	0.0083	0.0006	0.1470	0.0098	0.0011	0.437
1.915	0.213–0.804	0.233–0.733	0.0552	0.0542	0.0171	0.0007	0.1524	0.0181	0.0011	0.356
2.316	0.263–0.864	0.271–0.798	0.0523	0.0515	0.0177	0.0001	0.1621	0.0188	0.0008	0.317
2.707	0.304–0.825	0.326–0.769	0.0398	0.0388	0.0157	0.0008	0.1636	0.0173	0.0006	0.237
3.223	0.362–0.901	0.385–0.799	0.0322	0.0311	0.0152	0.0000	0.1697	0.0171	0.0005	0.183
3.871	0.438–0.893	0.463–0.762	0.0227	0.0206	0.0121	0.0002	0.1721	0.0150	0.0004	0.120
4.739	0.531–0.909	0.663–0.738	0.0145	0.0113	0.0081	0.0002	0.1684	0.0126	0.0002	0.067
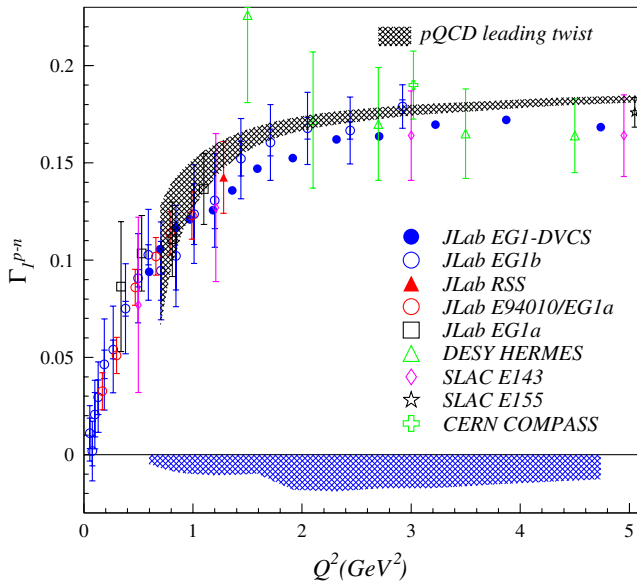
FIG. 1 (color online). The Bjorken sum Γ_1^{p-n}. The solid blue circles give our results. The blue band is the systematic uncertainty. Other symbols show the world data. For those, the inner error bar indicates the statistical uncertainty and the outer error bar the quadratic sum of the statistic and systematic uncertainties. The gray band represents the leading-twist NNLO pQCD calculation in the $\overline{\mathrm{MS}}$ scheme.
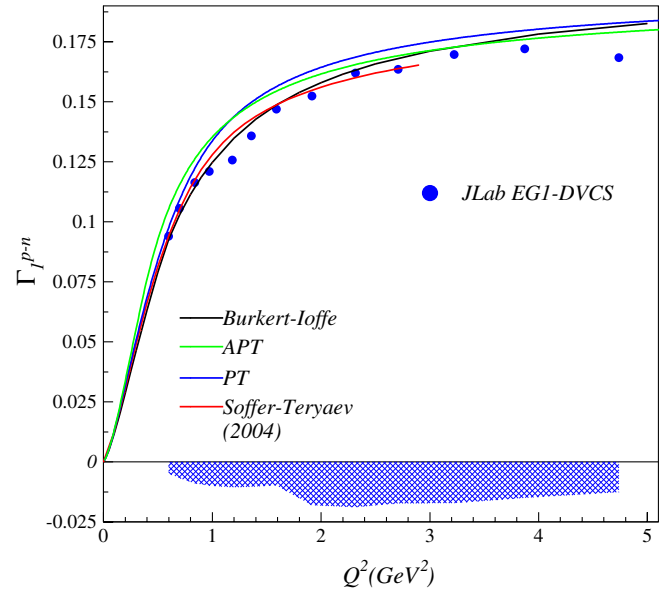

FIG. 2 (color online). The Bjorken sum Γ_1^{p-n} from EG1-DVCS (solid blue circles) compared with the phenomenological models described in the main text.

In order to evaluate the unmeasured parts of Γ_1^p and Γ_1^n at low x, we need a model for g_1^p and g_2^n covering a wide kinematic range. The model that we use here is built upon fits to the world data of the asymmetries A_1 and A_2, and the unpolarized structure functions F_1 and R. Those were modeled using a parametrization of the world data that fits both the DIS and resonance regions with an average precision of 2% to 3% [21]. The systematic uncertainty was calculated by varying either F_1 or R by the average uncertainty of the fit (2%–3%) and recalculating all quantities of interest.

For A_1 and A_2 we used our own phenomenological fit to the world data, including all DIS results from SLAC, HERA, CERN and Jefferson Lab and data in the resonance region from MIT Bates [22] and Jefferson Lab. The asymmetry A_2 in the DIS region was modeled using the Wandzura-Wilczek relation [23]. For systematic variations, we included a simple functional form for an additional twist-3 term introduced by E155 [5], and a model constrained by the Soffer bound [24].

At very low values of x, uncertainties in the model increase rapidly, so we imposed a lower limit at $x = 0.001$. Below this value, we extrapolate directly the isovector part of the structure function g_1 using the Regge parametrization $g_1^{p-n}(x) = g_1^{p-n}(x_0)(x_0/x)^{0.89}$. We chose the power 0.89 so that the Bjorken sum at $Q^2 = 5$ GeV^2 from the world data satisfies the Bjorken sum rule. Such a parametrization agrees within 50% with the low-x parametrization

determined in Ref. [25]. We assumed a 100% uncertainty on this contribution. The part below $x = 0.001$ contributes up to about 5% of the total sum.

EG1-DVCS does not cover the higher-x values. There, we used a fit to earlier JLab data [9,11].

The new determination of Γ_1^{p-n} is shown together with phenomenological models in Fig. 2. The Burkert-Ioffe model (black line) is an extrapolation of DIS data based on vector meson dominance, complemented by a parametrization of the resonance contribution [26]. The Soffer-Teryaev model (red line) uses the smoothness of $g_1 + g_2$ with Q^2 to extrapolate DIS data to lower Q^2 [27]. The two other lines are from Ref. [28]. They are updates of the Soffer-Teryaev model using standard perturbation theory (PT, blue line) and ghost-free analytical perturbation theory (APT, green line) which now includes the higher-twist terms μ_4 and μ_6. The higher-twist values were obtained from fits to the JLab data [18]. The APT formalism aims at reducing the influence of the Landau pole divergence at Λ_{QCD}.

The precision of the new determination of Γ_1^{p-n} allows us for the first time to see that the data lie systematically below the leading-twist NNLO pQCD prediction shown by the hatched band in Fig. 1. Although a large point-to-point correlated contribution to the systematic uncertainty could still make the data compatible with the leading-twist calculation, this difference and the steeper Q^2 evolution of the data compared to the leading-twist calculation for $Q^2 > 1.5$ GeV^2 suggest a negative higher-twist contribution to Γ_1^{p-n}. These features are quantitatively analyzed in the next section.

B. Higher-twist analysis

In this section, we determine quantitatively the higher-twist contributions to Γ_1^{p-n}. In addition to the EG1-DVCS data, we use all other world data, including the $Q^2 = 10$ GeV^2 SMC data [6] not visible in Fig. 1.

The moment Γ_1^{p-n} can be expanded in powers of $1/Q^2$; see Eq. (2). The coefficient of the first power correction is [29]

$$\mu_4^{p-n} = \frac{M^2}{9}(a_2^{p-n} + 4d_2^{p-n} + 4f_2^{p-n}), \qquad (3)$$

where M is the nucleon mass. The coefficient a_2^{p-n} is the twist-2 target mass correction expressed as

$$a_2^{p-n} = \int_0^1 dx(x^2 g_{1,LT}^{p-n}), \qquad (4)$$

in which $g_{1,LT}^{p-n}$ is the leading-twist part of g_1^{p-n}. The twist-3 matrix element d_2^{p-n} is given by

$$d_2^{p-n} = \int_0^1 dx x^2 (2g_1^{p-n} + 3g_2^{p-n}), \qquad (5)$$

and f_2^{p-n} is the twist-4 contribution to be extracted. These coefficients depend logarithmically on Q^2 but apart from f_2^{p-n}, we will neglect this small dependence in our analysis and use their values at $Q^2 = 1$ GeV^2. The leading order pQCD dependence of f_2^{p-n} is accounted for using its anomalous dimension [29]. The coefficient a_2 is a kinematical higher twist [30] containing no additional information than is provided by the leading-twist parton distributions. The dynamical higher-twist d_2 can be measured directly from polarized lepton scattering off transversely and longitudinally polarized targets. We are interested here in the dynamical higher-twist f_2 which can be obtained only from studying the Q^2 evolution of the moment of g_1.

For a consistent higher-twist analysis, the elastic contribution to Γ_1^{p-n} must be added [31] because it contains large higher-twist terms, as witnessed by the fast decrease of the elastic form factors with Q^2. At $Q^2 \sim 1$ GeV^2, the elastic contribution remains sizable and cannot be neglected. To determine it, we used the elastic form factor fits from Ref. [32] for the proton and Ref. [33] for the neutron. The strong coupling α_s enters in Eq. (2). We computed it in the $\overline{\text{MS}}$ scheme to next-to-leading order (β_1) in the α_s's β series. A fit of polarized parton distributions [34] was used to determine a_2^{p-n}. At $Q^2 = 1$ GeV^2, $a_2^{p-n} = 0.031 \pm 0.010$. The proton twist-3 d_2^p matrix element is obtained from [10]. Data from Refs. [10,19,35–37] and lattice calculations [38] suggest that for the neutron, d_2^n is negligible at $Q^2 > 2$ GeV^2. We use $d_2^n = 0.000 \pm 0.001$ at $Q^2 = 5$ GeV^2. Evolving d_2^{n-p} from $Q^2 = 5$ GeV^2 to 1 GeV^2 using the anomalous

dimension calculated in [29], we obtain $d_2^{p-n} = 0.008 \pm 0.0036$.

The world data on Γ_1^{p-n}, including those in Table I, except for the $Q^2 = 4.7$ GeV^2 point for which the estimated low-x contribution to the integral is large, were fit to extract f_2^{p-n} using Eqs. (2) and (3) with α_s, a_2^{p-n} and d_2^{p-n} determined as discussed above. To account for twist-6 and greater, we add a coefficient μ_6^{*p-n}/Q^4 to the fit. The asterisk reminds us that this coefficient includes not only the true μ_6^{p-n}/Q^4 correction, but also compensations for higher-order terms μ_N^{p-n} with $N > 6$. That is, $\mu_6^* = \mu_6 + \Sigma_{i=2,4,...}\mu_{i+6}/Q^i$. The equation shows explicitly that μ_6^* depends on Q^2 (beside its logarithmic dependence that we neglect). Approximating μ_6^* to be Q^2 independent is justified if the power series converges, and this should affect f_2 minimally but may lead to a μ_6^* significantly different from the actual μ_6. We have two completely free parameters, f_2 and μ_6^*, in the fit, plus a third parameter, the axial charge g_a, which is bounded by its experimental uncertainty range ($g_a = 1.27 \pm 0.04$).

As published, the world data on Γ_1^{p-n} are corrected for the missing low-x contribution using various estimates, depending on the publication. For the consistency of this analysis, the low-x estimates of the world data were recalculated using the model discussed in the Bjorken sum section. For all JLab data sets (Refs. [9,11] and the present data), the point-to-point uncorrelated uncertainties have been separated from the correlated ones using the *unbiased estimate*, and added in quadrature to the statistical uncertainties. The correlated systematics were propagated independently into the fit result, as was the uncertainty arising from α_s. The uncertainties stemming from a_2^{p-n} and d_2^{p-n} are negligible. Table II gives the best fits for several Q^2 ranges, since there is no prescription as to where in Q^2 the fit should start. The results are consistent. The first uncertainty listed is the quadratic sum of the statistical and point-to-point uncorrelated uncertainties. The second is the point-to-point correlated uncertainty. We do not report the parameter g_A in Table II. Its fit value is always $g_a = 1.305$, which corresponds to the upper bound of its variation range. This is due to the positive elastic contribution that dominates the Q^2 dependence of the sum for $Q^2 \lesssim 1$ GeV^2. For $Q^2 \lesssim 1$ GeV^2, the Q^2 dependence of the elastic contribution is less steep than that of the $1/Q^4$ or $1/Q^6$ higher-twist terms. These too-steep behaviors are compensated in the fits in part by a negative f_2^{p-n} and in part by an increased leading-twist contribution, i.e. by a larger g_A. This compensates for the too-steep Q^2 behavior of μ_6 or μ_8 compared to the data, since both the leading-twist and the f_2 contributions have slopes of opposite signs (their values increase with Q^2) to that of μ_6 or μ_8 (their values decrease with Q^2).

To assess the convergence of the twist series in Eq. (2), we give in Table III the best fits when an additional

TABLE II.   Values of f_2^{p-n} and μ_6^{*p-n} at $Q^2 = 1$ GeV^2 from the three-parameter fit (the parameter g_a is not reported in this table; see main text). The two uncertainties given for f_2^{p-n} and μ_6^{*p-n} are the point-to-point uncorrelated (first number) and point-to-point correlated uncertainties (second numbers). The last column gives the χ^2 per degree of freedom of the fit, with only the point-to-point uncorrelated uncertainties accounted for.

Q^2 range (GeV^2)	f_2^{p-n}	μ_6^{*p-n} (GeV^4)	χ^2/d.o.f
0.66–10.0	$-0.093 \pm 0.006 \pm^{0.026}_{0.037}$	$0.087 \pm 0.002 \pm^{0.033}_{0.022}$	1.03
0.84–10.0	$-0.064 \pm 0.009 \pm^{0.032}_{0.036}$	$0.070 \pm 0.004 \pm^{0.023}_{0.018}$	0.71
1.00–10.0	$-0.057 \pm 0.010 \pm^{0.039}_{0.043}$	$0.065 \pm 0.005 \pm^{0.021}_{0.019}$	0.72

TABLE III.   Same as Table II but for the four-parameter fit.

Q^2 range (GeV^2)	f_2^{p-n}	μ_6^{p-n} (GeV^4)	μ_8^{*p-n} (GeV^6)	χ^2/d.o.f
0.66–10.0	$-0.044 \pm 0.010 \pm^{0.055}_{0.054}$	$0.012 \pm 0.010 \pm^{0.024}_{0.034}$	$0.032 \pm 0.006 \pm^{0.023}_{0.017}$	0.63
0.84–10.0	$-0.035 \pm 0.015 \pm^{0.037}_{0.041}$	$-0.005 \pm 0.020 \pm^{0.008}_{0.009}$	$0.044 \pm 0.014 \pm^{0.019}_{0.010}$	0.66
1.00–10.0	$-0.020 \pm 0.032 \pm^{0.025}_{0.031}$	$-0.037 \pm 0.032 \pm^{0.019}_{0.019}$	$0.073 \pm 0.022 \pm^{0.018}_{0.013}$	0.67

μ_8^{*p-n}/Q^6 coefficient is used (the asterisk has the same meaning as for μ_6^*). In these four-parameter fits, μ_6 now gives more properly the $1/Q^4$ power correction. Similar convergence studies were done in [9] and [11], and results for μ_8^{*p-n} were consistent with zero with large uncertainties ranging from 0.04 to 0.09 depending on the Q^2 at which the fit starts. Now, the precision of the data allows us to determine the magnitude and sign of μ_8^{*p-n}. The question of the convergence of the higher-twist series arises naturally, since Refs. [9] and [11] indicated that μ_4^{p-n} and μ_6^{*p-n} are of similar magnitudes but opposite signs at $Q^2 \simeq 1$ GeV^2. This suggested a poor convergence of the twist series, at least in the Q^2 ranges concerned. With better data, it now appears that μ_8^{*p-n} and μ_6^{p-n} are of similar size while μ_6^{p-n} is small. This indicates that Eq. (2) converges only for $Q^2 \gtrsim 1$ GeV^2. The central value of μ_6^{p-n} is significantly smaller than that of μ_6^{*p-n}, once μ_8^{*p-n} is accounted for. However, μ_6^{p-n} and μ_6^{*p-n} are still compatible within uncertainties. A systematic study done with the models [26] and [27] is described in Ref. [39]. It was performed to better understand the convergence of the twist series given a truncation at μ_{max}^* (corresponding to μ_6^* for the three-parameter fit and to μ_8^* for the four-parameter fit) and a choice of Q_{min}^2, the lowest Q^2 used in the fit. The conclusion from the present experimental higher-twist extraction agrees with the model-based conclusions of Ref. [39]:

(i)   The extraction of f_2^{p-n} is stable as Q_{min}^2 and μ_{max} are modified in the ranges $0.6 \leq Q_{min}^2 \leq 3$ GeV^2 and $\mu_6^{p-n} \leq \mu_{max}^{p-n} \leq \mu_{12}^{p-n}$ for the model study, and in the range $0.6 \leq Q_{min}^2 \leq 1$ GeV^2 and with $\mu_{max}^{p-n} = \mu_6^{p-n}$ or μ_8^{p-n} for the present experimental study.

(ii) The coefficient μ_6^{p-n} is small, typically a factor of 6 smaller than f_2^{p-n} for the model and a factor of 3 smaller for the data, although a three-parameter fit

gives a larger μ_6^{p-n*} of similar magnitude to f_2^{p-n}. Increasing the number of parameters decreases μ_6^{p-n}. This implies the convergence of the series for $Q^2 \gtrsim 1$ GeV^2.

(iii) At $Q^2 \simeq 1$ GeV^2, there is an approximate cancellation of the higher-twist terms (independent of Q_{min}^2). The overall uncertainty on f_2^{p-n} is dominated by the unmeasured low-x region. The uncertainty from α_s becomes important only for fits starting at the lowest Q_{min}^2(0.66 GeV^2) since the effect of the Landau pole becomes important as Q gets close to Λ_{QCD}. The JLab data were all taken with beam energies of up to about 6 GeV. The upcoming 12 GeV program at Jefferson Lab will significantly reduce this dominant uncertainty since the measured fraction of Γ_1^{p-n} above $Q^2 = 2.5$ GeV^2 will at least double compared to the present measurement [40]. The twist-4 coefficient f_2^{p-n} obtained from the three-parameter fit over the 0.84–10 GeV^2 Q^2 range is plotted in Fig. 3 along with the results of Refs. [11] and [9] obtained
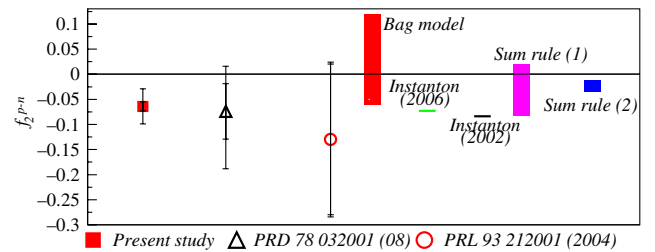

FIG. 3 (color online).   Three-parameter fit result for f_2^{p-n} from the present study (square) and Refs. [11] (triangle) and [9] (circle). The inner error bar represents the point-to-point uncorrelated uncertainty and the outer error bar is the quadratic sum of the point-to-point correlated and uncorrelated uncertainties. Theoretical calculations [41–44] are shown on the right.

using the same fit range, and theoretical predictions [41–44]. The magnitude and sign of f_2^{p-n} agree with the analysis performed on $g_1(x)$ in Ref. [45], which found that twist-4 corrections to $g_1(x)$ are sizeable but change sign at $x \sim 0.4$ for the proton, leading to a small integrated value. Our result expressed as $\mu_4^{p-n}/M^2 = -0.021 \pm 0.016$ (three-parameter fit with the 0.84–10 GeV^2 Q^2 range) also agrees with the several extractions done in Ref. [18], which are typically around $\mu_4^{p-n}/M^2 \sim -0.05$ with a spread of 0.02. Finally, our μ_4^{p-n}/M^2 is also in agreement with the higher-twist coefficients obtained in [46], which after integrating them over x yield $\mu_4^{*p-n}/M^2 = -0.058 \pm 0.045$.

C. Color electric and magnetic polarizabilities

The twist-3 and twist-4 terms of the μ_4 coefficient, Eq. (3), yield the color electric and magnetic polarizabilities [41,47], $\chi_E = \frac{2}{3}(2d_2 + f_2)$ and $\chi_B = \frac{1}{3}(4d_2 - f_2)$ respectively. Using the value of f_2^{p-n} from the three-parameter fit starting at $Q^2_{\min} = 0.84$ GeV^2 and $d_2^{p-n} = 0.0080 \pm 0.0036$, we obtain $\chi_E^{p-n} = -0.032 \pm 0.024$ and $\chi_B^{p-n} = 0.032 \pm 0.013$. The point-to-point correlated and uncorrelated uncertainties on f_2^{p-n} were symmetrized and added in quadrature. The polarizabilities are compatible with those reported in Ref. [11] with a factor of 2 improvement on the uncertainties.

D. The strong coupling α_s

The strong force coupling at the Z^0 pole, $\alpha_s(M_z^2)$, can be extracted from the Bjorken sum data by solving Eq. (2) for α_s, and then evolving α_s to the Z^0 pole. However, the relative uncertainty for this method is large, typically 30%, and dominated by the model determination of the unmeasured low-x region. Rather than using an absolute measurement, we can obtain $\alpha_s(M_z^2)$ more precisely by fitting the Q^2 dependence of Γ_1^{p-n} [48]. In our case, where we include relatively low Q^2 data points, we must account for μ_4^{p-n}. We can neglect the higher orders since μ_6^{p-n} is small and μ_8^{*p-n} is suppressed as $1/Q^4$ compared to μ_4^{p-n}. Since f_2^{p-n} was obtained assuming the validity of the Bjorken sum rule and using a theoretical α_s, we must use an independent determination of f_2^{p-n} to form μ_4^{p-n}. We choose f_2^{p-n} from Ref. [44], for which we assumed a 50% uncertainty. We used a $\overline{\text{MS}}$ leading-twist expression of Γ_1^{p-n} up to order α_s^5 and estimated the uncertainty due to the truncation of the leading-twist pQCD series by taking the difference between the fourth and fifth orders. We then evolved the extracted α_s to the Z^0 mass M_Z using the evolution equation up to order β_3 with $\Lambda_{\text{QCD}}^{\overline{\text{MS}}} = 0.214 \pm 0.070$ GeV.

Fitting the values of $\Gamma_{1,\text{tot}}^{p-n}$ in Table I, starting at $Q^2_{\min} = 2.316$ GeV^2 with g_A and Λ_{QCD} as fit parameters, we obtain $\alpha_s^{\overline{\text{MS}}}(M_Z^2) = 0.1123 \pm 0.0061$. The uncertainty is dominated by the point-to-point uncorrelated uncertainty ± 0.0050. The uncertainties from the truncation of the β series and from a_2^{p-n}, d_2^{p-n} and f_2^{p-n} are comparatively small. The point-to-point correlated uncertainty is ± 0.0037, which is dominated by the low-x estimate. To assess this point-to-point correlated uncertainty, we separated σ^{syst} in Table I into a constant with respect to Q^2, which does not contribute to the uncertainty on α_s, and a Q^2-dependent part. The latter is estimated by calculating $\Delta\Gamma = d(\Gamma_{1,\text{tot}}^{p-n})/dQ^2 \times (Q^2 \text{ bin size}) \times (\Gamma_{1,\text{tot}} - \Gamma_{1,\text{meas}})/\Gamma_{1,\text{tot}}$ for each Q^2 point. For this expression, the relative amount of the unmeasured low-x contribution, $(\Gamma_{1,\text{tot}} - \Gamma_{1,\text{meas}})/\Gamma_{1,\text{tot}}$, can be obtained from the last column of Table I. Each $\Delta\Gamma$ is treated as an additional uncertainty to Γ_1^{p-n} and is added in quadrature to the point-to-point uncorrelated uncertainty.

The Regge exponent determining the (small) contribution to the integral below $x = 0.001$ was obtained by assuming the validity of the Bjorken sum rule at $Q^2 = 5$ GeV^2. This implies evolving Eq. (1) from infinite Q^2 to $Q^2 = 5$ GeV^2. In the process, a value for α_s must be assumed. However, this initial assumption on α_s does not bias our determination of α_s. The contribution from $x < 0.001$ influences the absolute value of Γ_1^{p-n} at the few percent level. Our α_s depends on $x < 0.001$ only *via* the Q^2 dependence, for which we assigned the conservative uncertainty just discussed.

Our value of $\alpha_s^{\overline{\text{MS}}}(M_Z^2)$ is compatible with the average world data, $\alpha_s^{\overline{\text{MS}}}(M_Z^2) = 0.1185 \pm 0.0006$, and it significantly improves the precision on $\alpha_s^{\overline{\text{MS}}}(M_Z^2)$ from polarized DIS last reported by the Particle Data Group [49]. It is in excellent agreement with the result reported in Ref. [46], $\alpha_s^{\overline{\text{MS}}}(M_Z^2) = 0.1132^{+0.0056}_{-0.0095}$, extracted from the (noninte-grated) g_1 world data. Our result is less precise than direct measurements at the Z^0 pole, but has similar precision to some of the α_s results reported by the Particle Data Group. This demonstrates the viability of determining α_s with polarized DIS data, especially since, as already discussed for Γ_1^{p-n}, the leading uncertainty will be significantly reduced when the 12 GeV JLab data will become available [40] and *a fortiori* if the future polarized EIC becomes available [50].

III. SUMMARY

New JLab CLAS data have allowed us to form the Bjorken sum Γ_1^{p-n} for $0.60 < Q^2 < 4.74$ GeV^2. The sum is consistent with previous JLab data and exhibits a characteristically strong Q^2 behavior in the hadron-parton transition region. The statistical uncertainty is small compared to the systematic uncertainty, which is dominated by the contribution from the unmeasured low-x domain. While the analyses of former JLab data covered the low and intermediate Q^2 regions where hadronic degrees of freedom

play a role, the new data cover the intermediate and partonic (high Q^2) domains. This is particularly suited for extracting higher-twist coefficients and color polarizabilities. These quantities were extracted from a global analysis of the world data, including the new JLab data presented in this paper. The twist-4 coefficient was confirmed to be relatively large in absolute magnitude: $f_2^{p-n} = -0.064 \pm 0.036$ compared to the leading-twist coefficient $\Gamma_1^{p-n,\text{pQCD}} = 0.141 \pm 0.013$, the twist-2 coefficient $a_2^{p-n} = 0.031 \pm 010$, and the twist-3 coefficient $d_2^{p-n} = 0.008 \pm 0.003$. The net higher-twist effect is small around $Q^2 = 1$ GeV^2 because of a cancellation between twist-4 and the sum of higher power corrections that are of opposite sign. Fits with four parameters reveal that the twist-6 contribution is small and the cancellation comes from twist-8 and/or higher contributions. This implies the convergence of the twist series above $Q^2 \simeq 1$ GeV^2. The color electric and magnetic polarizabilities were extracted with a factor of 2 improvement on the uncertainty compared to earlier analyses. The two polarizabilities are of similar value but opposite sign. From the Q^2 behavior of Γ_1^{p-n} and a model estimate of f_2^{p-n}, we extracted $\alpha_s^{\overline{\text{MS}}}(M_Z^2) = 0.1123 \pm 0.0061$. The precision is a factor 1.5 better than earlier estimates from polarized DIS, making Γ_1^{p-n} a viable observable for determining α_s. Its agreement with the other α_s determined from different observables provides a consistency check of QCD.

[1] J. D. Bjorken, Phys. Rev. **148**, 1467 (1966); Phys. Rev. D **1**, 1376 (1970).

[2] P. L. Anthony *et al.*, Phys. Rev. Lett. **71**, 959 (1993); Phys. Rev. D **54**, 6620 (1996).

[3] K. Abe *et al.*, Phys. Rev. Lett. **74**, 346 (1995); Phys. Rev. Lett. **75**, 25 (1995); Phys. Rev. Lett. **76**, 587 (1996); Phys. Lett. B **364**, 61 (1995); Phys. Rev. D **58**, 112003 (1998).

[4] K. Abe *et al.*, Phys. Rev. Lett. **79**, 26 (1997); Phys. Lett. B **404**, 377 (1997); Phys. Lett. B **405**, 180 (1997).

[5] P. L. Anthony *et al.*, Phys. Lett. B **458**, 529 (1999); Phys. Lett. B **463**, 339 (1999); Phys. Lett. B **493**, 19 (2000); Phys. Lett. B **553**, 18 (2003).

[6] D. Adams *et al.*, Phys. Lett. B **329**, 399 (1994); Phys. Lett. B **336**, 125 (1994); Phys. Lett. B **357**, 248 (1995); Phys. Lett. B **396**, 338 (1997); Phys. Rev. D **56**, 5330 (1997).

[7] K. Ackerstaff *et al.*, Phys. Lett. B **404**, 383 (1997); Phys. Lett. B **444**, 531 (1998); A. Airapetian *et al.*, Phys. Lett. B **442**, 484 (1998); Phys. Rev. Lett. **90**, 092002 (2003); A. Airapetian *et al.*, Phys. Rev. D **75**, 012007 (2007).

[8] V. Yu. Alexakhin *et al.*, Phys. Lett. B **647**, 8 (2007); M. G. Alekseev *et al.*, Phys. Lett. B **690**, 466 (2010).

[9] A. Deur *et al.*, Phys. Rev. Lett. **93**, 212001 (2004).

[10] F. R. Wesselmann *et al.*, Phys. Rev. Lett. **98**, 132003 (2007); K. Slifer *et al.*, Phys. Rev. Lett. **105**, 101601 (2010).

[11] A. Deur *et al.*, Phys. Rev. D **78**, 032001 (2008).

[12] J.-P. Chen, A. Deur, and Z.-E. Meziani, Mod. Phys. Lett. A **20**, 2745 (2005).

[13] A. L. Kataev, Mod. Phys. Lett. A **20**, 2007 (2005).

[14] M. Göckeler, R. Horsley, D. Pleiter, P. E. L. Rakow, A. Schäfer, and G. Schierholz, Nucl. Phys. B, Proc. Suppl. **119**, 32 (2003).

[15] V. D. Burkert, Phys. Rev. D **63**, 097904 (2001).

[16] Y. Prok *et al.* (CLAS EG1-DVCS Collaboration), arXiv:1404.6231.

[17] J. Ellis, E. Gardi, M. Karliner, and M. A. Samuel, Phys. Lett. B **366**, 268 (1996).

[18] K. A. Milton, I. L. Solovtsov, and O. P. Solovtsova, Phys. Lett. B **439**, 421 (1998); R. S. Pasechnik, D. V. Shirkov, and O. V. Teryaev, Phys. Rev. D **78**, 071902 (2008); R. S. Pasechnik, D. V. Shirkov, O. V. Teryaev, O. P. Solovtsova, and V. L. Khandramai, Phys. Rev. D **81**, 016010 (2010).

[19] M. Amarian *et al.*, Phys. Rev. Lett. **92**, 022301 (2004).

[20] M. Lacombe, B. Loiseau, J. Richard, R. Mau, J. Côté, P. Pirès, and R. de Tourreil, Phys. Rev. C **21**, 861 (1980); R. Machleidt, K. Holinde, and C. Elster, Phys. Rep. **149**, 1 (1987); M. J. Zuilhof, and J. A. Tjon, Phys. Rev. C **22**, 2369 (1980); K. Kotthoff, R. Machleidt, and D. Schutte, Nucl. Phys. **A264**, 484 (1976); B. Desplanques, Phys. Lett. B **203**, 200 (1988).

[21] M. E. Christy and P. E. Bosted, Phys. Rev. C **81**, 055213 (2010).

[22] O. Filoti, Doctoral dissertation, University of New Hampshire, 2007.

[23] S. Wandzura and F. Wilczek, Phys. Lett. B **72**, 195 (1977).

[24] J. Soffer, Phys. Rev. Lett. **74**, 1292 (1995).

[25] S. D. Bass and M. M. Brisudova, Eur. Phys. J. A **4**, 251 (1999).

[26] V. D. Burkert and B. L. Ioffe, Phys. Lett. B **296**, 223 (1992); J. Exp. Theor. Phys. **78**, 619 (1994).

[27] J. Soffer and O. V. Teryaev, Phys. Lett. B **545**, 323 (2002); Phys. Rev. D **70**, 116004 (2004).

[28] R. S. Pasechnik, J. Soffer, and O. V. Teryaev, Phys. Rev. D **82**, 076007 (2010).

[29] E. V. Shuryak and A. I. Vainshtein, Nucl. Phys. **B201**, 141 (1982); X. Ji and P. Unrau, Phys. Lett. B **333**, 228 (1994); H. Kawamura, T. Uematsu, Y. Yasui, and J. Kodaira, Mod. Phys. Lett. A **12**, 135 (1997).

[30] J. Bluemlein and A. Tkabladze, Nucl. Phys. **B553**, 427 (1999).

[31] X. Ji, Phys. Lett. B **309**, 187 (1993); X. Ji and W. Melnitchouk, Phys. Rev. D **56**, R1 (1997).

[32] J. Arrington, W. Melnitchouk, and J. A. Tjon, Phys. Rev. C **76**, 035205 (2007).

[33] P. Mergell, U.-G. Meissner, and D. Drechsel, Nucl. Phys. **A596**, 367 (1996).

[34] J. Bluemlein and H. Boettcher, Nucl. Phys. **B636**, 225 (2002).

[35] X. Zheng *et al.*, Phys. Rev. C **70**, 065207 (2004).

[36] P. Solvignon *et al.*, arXiv:1304.4497.

[37] M. Posik *et al.*, Phys. Rev. Lett. **113**, 022002 (2014).

[38] M. Göckeler, R. Horsley, W. Kürzinger, H. Oelrich, D. Pleiter, P. Rakow, A. Schäfer, and G. Schierholz, Phys. Rev. D **63**, 074506 (2001).

[39] A. Deur, JLab report, http://tnweb.jlab.org/tn/2008/08-001.pdf.

[40] S. Kuhn *et al.*, CLAS12 Experiment E-12-06-109, www .jlab.org/exp_prog/proposals/06/PR12-06-109.pdf.

[41] E. Stein, P. Górnicki, L. Mankiewicz, and A. Schäfer, Phys. Lett. B **353**, 107 (1995).

[42] I. I. Balitsky, V. M. Braun, and A. V. Kolesnichenko, Phys. Lett. B **242**, 245 (1990); I. I. Balitsky, M. Beneke, and V. M. Braun, *ibid.* **318**, 648(E) (1993).

[43] N. Y. Lee, K. Goeke, and C. Weiss, Phys. Rev. D **65**, 054008 (2002).

[44] A. V. Sidorov and C. Weiss, Phys. Rev. D **73**, 074016 (2006).

[45] E. Leader, A. V. Sidorov, and D. B. Stamenov, arXiv:hep-ph/0612360.

[46] J. Bluemlein and H. Boettcher, Nucl. Phys. **B841**, 205 (2010).

[47] X. Ji, arXiv:hep-ph/9510362.

[48] G. Altarelli, R. D. Ball, S. Forte, and G. Ridolfi, Nucl. Phys. **D496**, 337 (1997).

[49] C. Amsler *et al.* (Particle Data Group), Phys. Lett. B **667**, 1 (2008).

[50] A. Accardi *et al.*, arXiv:1212.1701.